Studies on Operation of Large Scale Solar Flat Plate Reflecting System and Its Thermal Performance

A Ph.D. Synopsis submitted to The Maharaja Sayajirao University of Baroda in fulfilment of the requirements of the degree of

Doctor of Philosophy
in
Mechanical Engineering

By

Mr. Jay I. Patel
(Reg. No: FOTE/1071)
PhD Scholar

Under supervision of

Dr Amit R. Patel,
Associate Professor

Mechanical Engineering Department,
Faculty of Technology and Engineering
The Maharaja Sayajirao University of Baroda
Vadodara
January 2024

Abstract

Performance of a solar reflector depends upon the topology of the reflector unit. Curved reflectors undoubtedly exhibit superior performance characteristics, but they are burdened with high costs, intricate manufacturing processes, and often rely on non-indigenous technology for production. Conversely, flat plate solar reflecting systems (FPSRS) offer a cost-effective solution, widespread availability, and are inherently indigenous in nature. Present study presents a methodology to evaluate various configurations of large-scale FPSRS under azimuthal sun alignment. The suggested method entails evaluating each ray's performance after it has been reflected by many FPSRS reflectors. A small-scale model of a square-type configuration (STC) based FPSRS was built and tested utilising laser light in a controlled dark room environment to validate this technology. The FPSRS is a solar reflector with a funnel shape that resembles the inverted frustum of a square pyramid. Rays were categorized into six distinct categories, ranging from case A to case F, to enhance our understanding of its behaviour. The intersection point on the reflector is meticulously recorded for subsequent analysis. Furthermore, an uncertainty analysis of the experimental setup is conducted to quantify the impact of manufacturing variations when scaling up the unit. The results of the uncertainty analysis for the FPSRS indicate that the maximum uncertainty (χ) in the ray path is 2.96%, considering a ± 1° manufacturing error. The experimental findings obtained through the single-ray experimental approach are validated by comparing them to an earlier shadow experiment involving a solar system-augmented flat reflector designed for thermal applications, as conducted by A. C. Andres et al. [1]. The validated results unequivocally establish that the currently proposed experimental procedure surpasses traditional approaches in terms of both reliability and feasibility. Nevertheless, the results obtained from the experimental analysis of the ray path were cross-validated with a CAD model of similar dimensions to the FSRU. This validation process revealed a maximum deviation (δ_{max}) in the path of 2.1% between the CAD model and the experimental results.

The numerical model of FPSRS is made with use of the ray tracing algorithm (RTA) in MATLAB software. Equations for solar radiation and three-dimensional geometrical equations are used to build the RTA. A two-step guideline is used to establish grid independence: (1) length of characteristic (LC) and effective grid reduction ratio (EGR) approaches are used to (1) identify a crucial grid refinement region, and (2) compute the optimal grid number utilising CVRMSE and R2 coefficient of determination analysis. The RTA is subsequently validated against experimental results and employed for optimizing geometry with diverse solar radiation inputs. Comparative analysis reveals a 2.9% variation in ray distribution profile (RDP) at the base receiving surface (BRS) and a 3.2% change in optical efficiency (η_{opt}). These findings affirm RTA's suitability for further topological optimization. Furthermore, the RTA analyses the impact of (i) height-to-bottom (H/B) ratio, (ii) reflector angle relative to the horizontal surface, and (iii) different aperture areas on FSRU's optical performance. Using numerical methods and considering various atmospheric conditions during summer and winter solstices, optimal H/B ratios between 1.52 and 2 are identified for peak FSRU performance. The RTA analysis compared octagonal type configuration (OTC) and hexagonal type configuration (HTC) for varying solar radiation conditions. Results indicate superior performance of aperture-based designs over STC, with OTC showing a 5.1% advantage in RDP for lower altitude solar rays, offering cost-effective manufacturing.

List of Figures

List of Tables

Nomenclature

Symbol	**Description**
A_a	Absorber area (m^2)
B	Length of the single side of the BRS (m)
G_{sc}	Extra-terrestrial radiation incident outside of the earth (W/m^2)
H	Vertical height of the FPSRS (m)
N	Optimum grid number
N_{Cell}	Number of cell on the TIS
N_{TIS}	Number of rays incoming from the TIS
R^2	Coefficient of determination (-)
u	Normal to the plane (-)
Greek letter	
α_h	Angle made by reflector to the horizontal plane (%)
β	Angle of the slope (%)
Φ	Angular location north or south of the equator (%)
δ	Declination angle (%)
δ_E	Error (%)
ω	Hour angle (%)
χ	Maximum uncertainty (--)
η_{opt}	Optical efficiency (%)
θ	Solar incident angle (%)
γ_Z	Surface azimuthal angle (%)
Abbreviation	
BRS	Bottom receiving surface
CVRMSE	Coefficient of variation of root-mean-square error
EGR	Effective grid reduction ratio
FPSRS	Flat plate solar reflecting system
HTC	Hexagonal type configuration

LC	Length of characteristic
OTC	Octagonal type configuration
RDP	Ray distribution profile
RTA	Ray tracing algorithm
SS	Summer solstice
STC	Square type configuration
TIS	Top imaginary surface
WS	Winter solstice

Table of contents

Chapter 1 Introduction

1.1 Motivation and Background

Energy is indispensable in every sector of society, spanning from cooking, heating, cooling, lighting, transportation, and operating appliances to information technology, communication, and machinery. However, ensuring access to reliable and clean energy has become a challenging task for global development and the well-being of humanity [1]. According to the international energy agency (IEA), worldwide energy consumption will rise by 4.6% in 2021 and expected to rise in further year but the supply of non-renewable energy sources will decrease dramatically [2]. Under this scenario, the use of renewable energy sources especially solar energy is an attractive alternative for the country. The usage of solar thermal energy is widespread and may be utilised for many different things, including steam generation in power plants, cooking, drying, and boiling water. Most of the solar thermal system has two main parts; a solar reflector and a receiver. There are two variants of reflectors are in the present use (a) curved type reflector and (b) flat plate type reflector. The curved type reflectors can concentrate the sun light at the focal point in more effective manner. However, to achieve high degree of concentration the precise solar tracking system is essential [3]. In addition, manufacturing curved reflectors at a higher cost than flat plate counterparts is a disadvantage, especially for a nation like India. On other hand the use of flat plate reflector is less costly but at the same time it is less efficient. Selecting correct combination, considering trade-off between cost and efficiency, is a real challenge for designing a cost efficient system. In the following discussion, the litrature use for the exploring the flat plate refelctor and its application followed by the reserch gap and possilbe solution is discussied.

1.2 Literature review

Present section discuss about the literatures refereed for the basic understanding of the contribution made by flat plate solar reflecting system (FPSRS). By reviewing the open literature it is observed that that the use of flat plate reflectors are well established, however the applications involving large size flat plate reflectors are scares [4]. A systematic study of determining the performance for such applications for a large size can certainly change the scenario. However very few literature attempt numerical analysis of a trajectory of ray for a single heliostat reflector or flat plate reflector for the solar application. Detailed study of solar funnel cooker (SFC), as an additional reflector unit, for low sun elevation and sun light had been carried out by C. R. Ruvio et al. [5] assuming the consideration of azimuthal solar tracking method. The results shows that thermal performance is increased about 24% compared to a normal solar cooker. Few studies developed a numerical model to analyse the performance of similar reflector unit using the concept of ray tracing. In another approach the area of the shadow casted by an inclined reflector is considered as an indication of intensity of the radiation. The use of the normal optical tracing or shadow is not novel as it has been used by certain commercial software and one of such application is demonstrated by A. Carrillo et al. [6]. They have carried out investigation using ray tracing simulation software (*Soltrace*® *& Transys*®) by considering four different models of SFC. However, William

Brandley [7] carried out the numerical investigation of multiple reflectors by ray tracing approach. Under this study the rays are not received but released from the centre of the solar cooker and its interaction with various reflector are studied. However above all studies are based on the shadows of the ray's reflection on the receiving surface and its effect it analysed where the analysis of single ray's behaviour after the reflection is yet to remaining.

In addition, the impact of increase in the number of reflectors on the performance of solar cooker is experimented by H. M. Wassie et al. [8] under full loading and without loading condition. The cooker with a three-sided reflector came out with the most effective results and was ideal for cooking Ethiopian cuisine, according to the findings. The experimental investigation on the single pass air heater with integrating two mirror type flat plate reflectors is carried out A. S. Abdillah et al. [9]. The results shows that the system's thermal efficiency increases by 12% in case of modified system. In a similar experimental investigation carried out by H. Baumik et al. [10], a flat reflector was utilised in conjunction with a solar water collector to examine its impact on both the economics as well as overall effectiveness of the collection. The study's findings indicate that the collector's total effectiveness outweighs the expense of the additional reflector. H. Tanaka [11] conducted a theoretical analysis of the bottom flat plate reflector's impact on the performance of the solar thermal collector and arrived to the following two conclusions: (1) the incremental angle of the reflector with the horizontal and (2) decreasing the gap between the collector and the reflector aid in improving system efficiency.

However, literature also cautioned that under certain cases the result obtained by these commercial software disagree to a great extent with their theoretical predictions. The large error observed while validating with experimental results, that is predicted by researchers in their respective research which emphasises a need to propose a simplified and reliable testing procedure. To overcome this issue of such discrepancies or deviations in the results and to obtain the first-hand data, the experiment was carried out by S more et al. [12] is very relevant for developing a testing facility dedicated to a curved reflector geometry. Under this study they created a dedicated and simple testing facility and carried out experiments to test a compound parabolic concentrator (CPC) using laser as a light source. The path traced by the ray of the light (laser in their case) is systematically tracked.

1.3 Problem formulation and objective

Literature review confirm that curved type of the reflector required precise tracking system to get optimum efficiency of the solar reflecting system. Additionally, the manufacturing cost and the availability of the curved type reflector (CTR) in the local market at reasonable price is added more challenges. However, the counter part of CTR based solar reflecting system, the flat plate type reflecting (FTR) solar system performed better and in the large scale its good alternative to the CTR solar system. Besides, the manufacturing cost of the FTR is very low and it's easily available in the local market. Also there is little tracking is needed in the FTR augmented solar thermal system. But there is no proper study found on the large application of the FPSRS as well as no dedicated numerical solver/software to predict the performance of the single ray behaviour after it het multiple reflection from the different angled flat reflectors. Additionally, there is lacuna in the availability of dedicated methodology

for examine the behaviour of the single ray. However, fewer studies demonstrate the experimental as well as numerical investigation of the multiple heliostat reflector and its thermal performance.

Literature demonstrate that use of large size FPSRS can be ground breaking application for the large size community hall and as a heat source. As minor tracking (azimuthal alignments) can work better for optimum thermal efficiency. Additionally, the study about the ray and its behaviour on the reflection on the FPSRS can be good output for large application. The optimisation of the FPSRS can give better edge to the performance of the solar thermal system. By changing the top aperture area from square type from square to hexagonal, octagonal will impose great impact on the optical performance of the system.

Based upon the literature survey, the following research gaps are identified:

- There is need to move from conventional curved type of solar reflecting system to new flat plate type of solar reflecting system.
- A need to develop azimuthal aligned flat plate type solar reflecting system for understanding the behaviour of the reflected rays.
- There is a need of develop an experimental and numerical mythology to deciding the effect of reflection on the performance of the ray and the path it travelled.
- A need to develop a numerical solver/software based on the ray tracing algorithm (RTA) to analyse the optical and thermal performance of the FPSRS.

From the above mentioned research gap the formulation of the problem and the proposed methodology is discussed here in. The use of FPSRS for large application can be very cost effective alternative to the costly CTR based solar reflecting system. The understanding of the ray behavioural pattern after the reflection from the reflector is played very important role increasing the optical and thermal performance of the system. Additionally, availability of the numerical solver/software to predict the performance of the ray and its interaction with flat plate reflector benefited in number of ways to improve the optical efficiency of the system. The development of methodology for understanding the ray's behaviour and analysing with experimental and numerical method has been chose for the present study to explore.

Based upon above research gaps and problem statement, the following objectives have been chosen for the present study,

- To develop and optimize a scaled-down model of a flat plate reflector system with multiple reflectors and test the single-beam-type ray testing methodology.
- To analyze and validate the proposed testing methodology using a generalized ray tracing algorithm for tracking a single ray undergoing multiple reflections.

1.4 Synopsis outline

Present chapter discuss about the introduction and motivation of the solar thermal system used flat plate reflectors. The brief literature review with highlights different methods used for solar thermal application with use of flat plate reflector are demonstrated. The research gap, formulation of the problem and objectives are presented after the literature review. Chapter 2 discuss the proposed mathematical and numerical modelling of the FPSRS in details. Additionally, the guidelines for the grid independent test for the time and space dependent parameter is presented after the modelling of the FPSRS. However chapter 3 describes the details of the experimental setup and the process follow to perform the experiment. The CAD modelling of the square type aperture area based FPSRS system is presented for better understanding of the path follow by the ray and to validate with the experimental setup. Additionally, the uncertainty analysis of the present experimental setup is also discuss in the present section. Chapter 4 discuss about the results obtained from the experimental and numerical investigation. First the validation of the experimental results with previously performed experiment with the similar kind of the setup id done. Additionally, the validation of the experimental results with the RTA is also demonstrated in the present section for the variable of the ray distribution profile of the ray and the optical efficiency. Chapter 5 demonstrate the conclusion of the present work and the future scope of it.

Chapter 2 Mathematical and numerical modelling

2.1 Mathematical modelling

Mathematical formulation and the steps used for tracing a particular ray is discussed herein. The derived equations used of solar radiation and analytical solid geometric to develop the mathematical model are presented in present section. The solar incident angle with the reflecting surface is obtain from the Eq. (1), where Φ is the angular location north or south of the equator, δ is the declination angle, β is the angle of the slope, γ_Z is the surface azimuthal angle, ω is the hour angle and θ is the solar incident angle.

$$\cos\theta = \sin\emptyset(\sin\delta \cdot \cos\beta + \cos\delta \cdot \cos\gamma \cdot \cos\omega \cdot \sin\beta) + \cos\emptyset(\cos\delta \cdot \cos\omega \cdot \cos\beta - \sin\delta \cdot \cos\gamma \cdot \sin\beta) + \cos\delta \cdot \sin\gamma \cdot \sin\omega \cdot \sin\beta \quad (1)$$

The equation of the line is obtained is obtained from the following (Eq. (2)) where, t is the constant use to define the intersection point on the line and the location of intersection point is represented with x, y, z. However x_1, y_1, z_1, and x_2, y_2, z_2 are the starting and end point of the line. Similarly, the pane equation is get from the Eq. (3), where a, b, and c are the coefficient to the normal of the plane.

$$\text{line equation can be represented as, } (0 \le t \le 1)\begin{cases} x = x_2 + (1 - x_2)t \\ y = y_2 + (1 - y_2)t \\ z = z_2 + (1 - z_2)t \end{cases} \quad (2)$$

$$\text{Plane equation can be represented as, } a(x - x_0) + b(y - y_0) + c(z - z_0) = 0 \quad (3)$$

The normal of the plane (u) is get from the Eq. (3) and the angle between two lines is calculated from Eq. (4) where, l, m, n are the coefficient between the two intersecting line. The equations and the steps are used to compute the path of the ray is explained in the following section with use of Fig. 1. Detailed expression to represent plane, line, solar incident angle, intersection point of line with plane, etc. during traversing for a typical ray is as shown in Fig. 1. The basic schematic of the ray travelling from the top imaginary surface (TIS) to the BRS and the path follow by the single ray is shown in the Fig. 2(a). However, the TIS of the reflector is discretized in several small areas as shown in Fig 2 (b).

$$\text{Normal to plane (u)} = \begin{bmatrix} i & j & k \\ u1 & v1 & z1 \\ u2 & v2 & z2 \end{bmatrix} \quad (4)$$

$$\text{Angle between two lines } \cos\theta = \frac{l_1 l_2 + m_1 m_2 + n_1 n_2}{\sqrt{(l_1^2 + m_1^2 + n_1^2}.\sqrt{(l_2^2 + m_2^2 + n_2^2}} \quad (5)$$

2.2 Numerical modelling

The numerical methods used to analyse the behaviour of beam rays arriving from the TIS and entered to the system for various atmospheric circumstances, are explained in the present section. A single ray's behaviour may be theoretically anticipated, specialised numerical modelling is necessary to comprehend the interaction of several

rays coming from the TIS. For a better understanding of ray and reflector interaction, the rays are considered to be lines and the reflector is a planar surface. Figure 2 (b) shows the marching direction of the core point for consideration of RTA for the case of HTC based FPSRS.

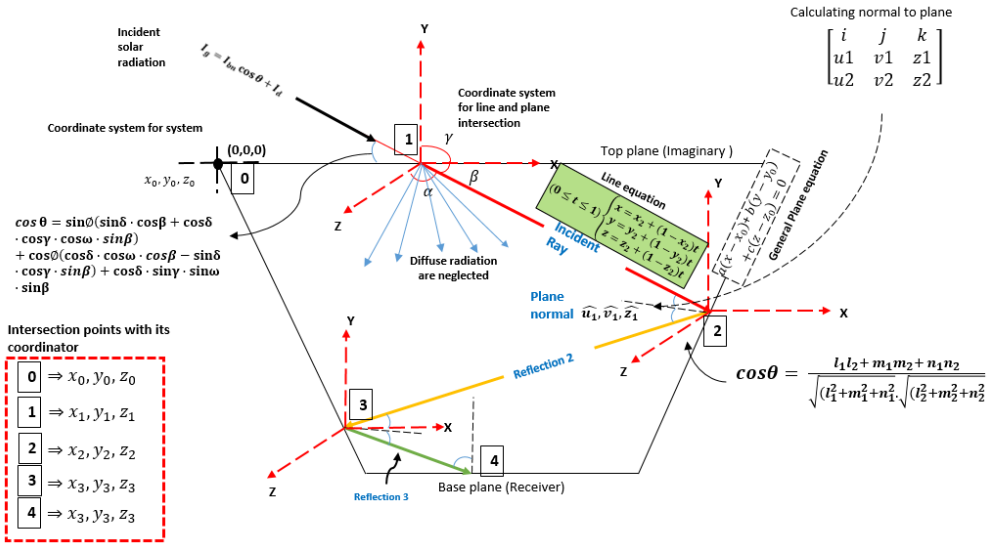

Fig. 1 Mathematical description of the solar reflector configuration considered for the study (Red, green and yellow colour lines shows the degradation of ray intensity)

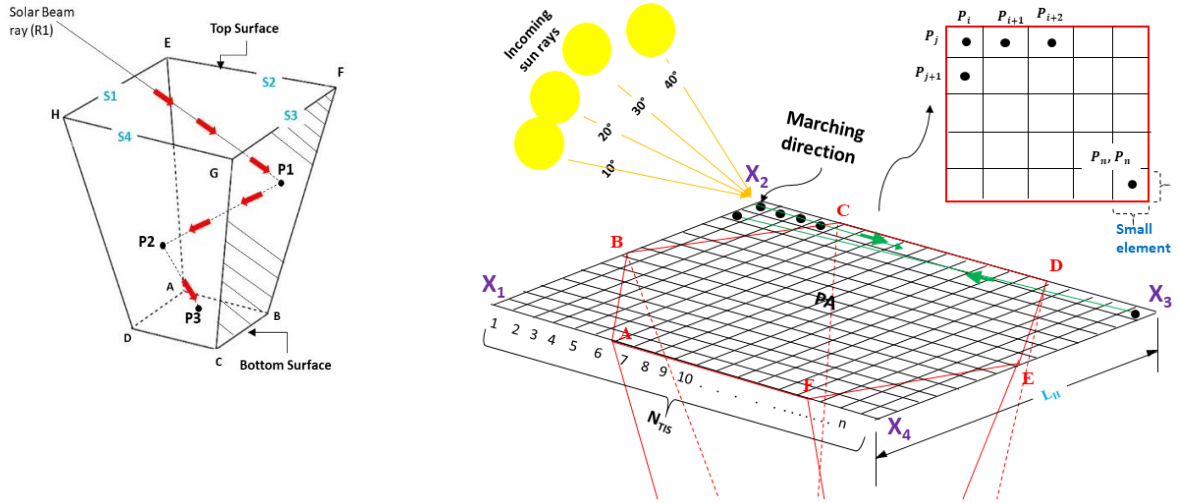

(a) (b)

Fig. 2 (a) Path follow by the ray after the reflection from the reflector and (b) marching direction of the core point on the TIS.

The total aperture area and the actual participating area are distinguished using a specific coordinate system, as illustrated in the figure. Additionally, the following coordinates represent the non-participating areas: (i) X_1, B and A, (ii) X_2, B and C, (iii) X_3, D and E, and (iv) X_4, F and E. In order to accommodate for minor components, the graphic also shows the i, j, and k coordinates of the TIS and the green colour line shows the marching direction

of the RTA when its application for the simulation. It enables a more complete knowledge of the system's performance by allowing us to recreate and examine the behaviour of rays in complex surroundings. The mathematical basis for this study is provided by the use of line and plane equations, which makes it easier to anticipate ray paths and interactions with the reflector.

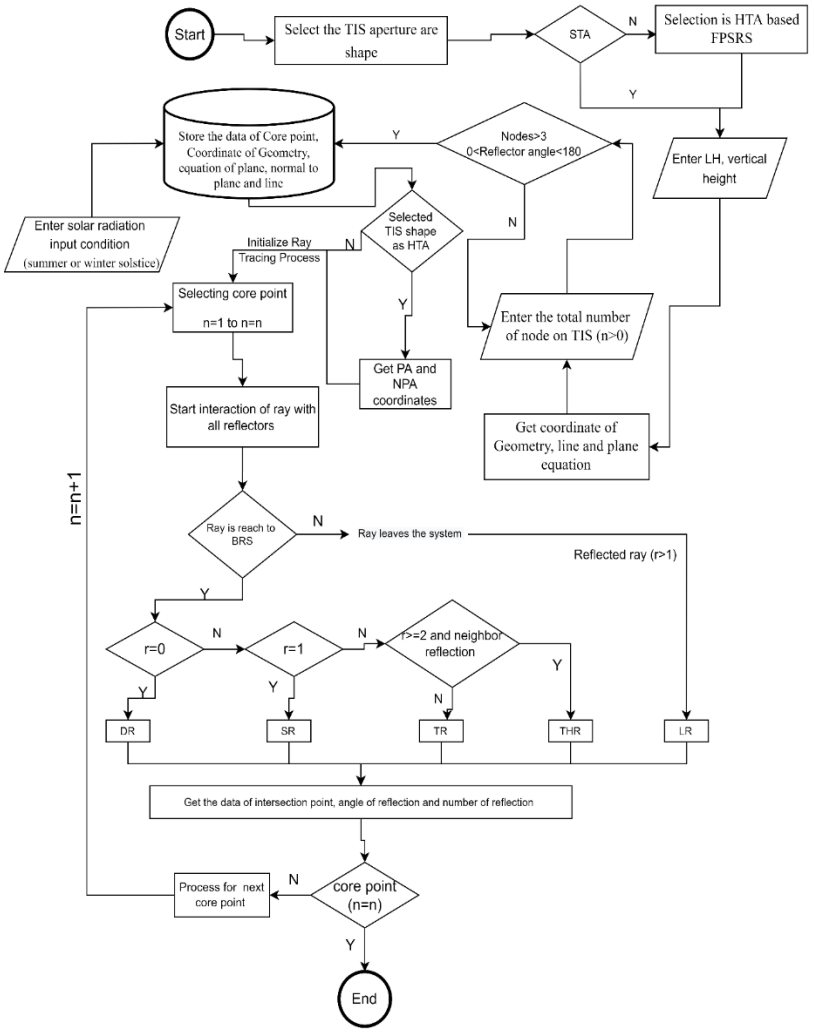

Fig. 3 Ray tracing algorithm for predicting the behaviour of solar ray.

Fig. 3 illustrates the RTA and it is developed using derived solar radiation and three-dimensional geometric analytical equations (see Eq. (1) to (5)). The RTA serves to understand the behaviour of each ray after it gets reflected from the reflectors and is examined using MATLAB software. Initially, the computation starts by entering the geometric data (STC or HTC-based FPSRS) and solar data as the primary input conditions. Next, the total number of nodes is intentionally set to more than one node to avoid inline errors on the TIS, and the reflected angle (Φ) is constrained to be between 0° to 180°, considering the maximum possible movement of the sun over the earth. Once all input conditions are entered, the algorithm stores all reflecting plane equations, their coordinates, and the normal equations of each plane. The ray tracing simulation then begins by considering each core point incrementally until all points are accounted for in this process (refer Fig. 2(b) for the incremental arrangement of core points). Subsequently, each ray starts to interact with the reflector and either reaches to the

BRS or leaves the system through the TIS. The algorithm continues by selecting the next core point from the TIS for simulation, repeating this process until all core points are considered, ultimately leading to the termination of the algorithm.

2.3 Guidelines for optimum gird for FPSRS

Present section discuss the solution-based guideline to determine the ideal number of grid points (N) for FPSRS. The proposed guidelines have two steps where in the first step, the length of characteristic (LC) and effective grid reduction ratio (EGR) methods have been used to quickly locate a region where refinement of grid number is wanted or is critical and improvement in this region would help reduce the error. By quickly detecting essential regions, it also cuts down on the amount of time the grid refinement process takes to compute. The right value of optimum grid number (N) is discovered in the second stage using the coefficient of variation of root-mean-square error (CVRMSE) and the coefficient of determination (R^2) approaches. Hence the LC and the EGR are worked as the *"indicative methods"* and the CVRMSE and the R^2 are worked as the *"deterministic methods"*. The Eqs. from (6) to (8) are being used to find out the sample getting selected (P), Sample variance (σ) and Population mean ($\bar{X}$) are mentioned below [14]. Here, N_n is represent the total number of sample taken for study and n is the sample size.

$$P = 1 - (1 - \frac{1}{N_n})n \tag{6}$$

$$\sigma^2 = \frac{\sum_{i=1}^{N}(X_i - \bar{X})^2}{N_n} \tag{7}$$

$$\bar{X} = \frac{\sum_{i=1}^{N} X_i}{N_n} \tag{8}$$

The mathematical description of EGR is as shown in Eq. 9 while the ration of two successive grid number is defined by Normal Grid Reduction Ration (NGRR) which can be obtained from Eq. 10. The LC of the variable can be obtain from the Eq. 11. However, the RMSE and CVRMSE can be get from the use of Eq. 12 and Eq. 13. The value of the R^2 is obtained from the Eq. 14.

$$EGR = \left(\frac{N_1}{N_2}\right)^{(1/d)} \tag{9}$$

$$\text{NGRR} = \frac{N_1}{N_2} \tag{10}$$

$$LC = \frac{Grid\ Resolution}{\max of\ [dx\ or\ dy]} = \frac{R}{W} \tag{11}$$

$$RMSE = \sqrt{\frac{\sum_{i=1}^{N}(M_i - S_i)^2}{M_i}} \tag{12}$$

$$CVRMSE = \frac{1}{N_i}\sqrt{\frac{\sum_{i=1}^{N}(M_i - S_i)^2}{M_i}} \tag{13}$$

$$R^2 = 1 - \frac{\sum_i (M_i - S_i)^2}{\sum_i (M_i - \bar{M}_i)^2} \tag{14}$$

The grid refinement process can be suggested in terms of following generic steps:

Step 1, apply indicative methods (LC or EGR) to obtain the zone of grid refinement.

Step 2, apply deterministic methods (CVRMSE or R^2) to obtain exact number of N.

The five different position of grid points (space variation) as well as at seven different positions of the sun positions during the day (time variation) as shown in the Table 1. Each combination of test run is identified with a particular tag. During the analysis, the following quantities are kept constant: α is kept 60°, θ is 30°and δ = 22.36°. The solar radiation intensity corresponding to 30° is 149 W/m^2. The value of *N* obtained after successful implementation of step1 is in the range of 1200 to 1700, by following the condition of EGR and in the range of 1500 to 1700 by following the condition of LC respectively (See Fig. 4(a) and Fig. 4(b)). However, the value of the N will be 1681after implementing step 2 according to the guidelines.

Table 1 Different positions of grid and different instances of ray

Cases	**Angle & Tag**						
Position & Tag	(30˚), 1	(40˚), 2	(50˚), 3	(60˚), 4	(70˚), 5	(80˚), 6	(90˚), 7
(i_{-2}), A	A1	A2	A3	A4	A5	A6	A7
(i_{-1}), B	B1	B2	B3	B4	B5	B6	B7
(i_0), C	C1	C2	C3	C4	C5	C6	C7
(i_{+1}), D	D1	D2	D3	D4	D5	D6	D7
(i_{+2}), E	E1	E2	E3	E4	E5	E6	E7
(i_{avg}),* F	F1	F2	F3	F4	F5	F6	F7

Note: * Position F corresponds to average of all the values of position A to E.

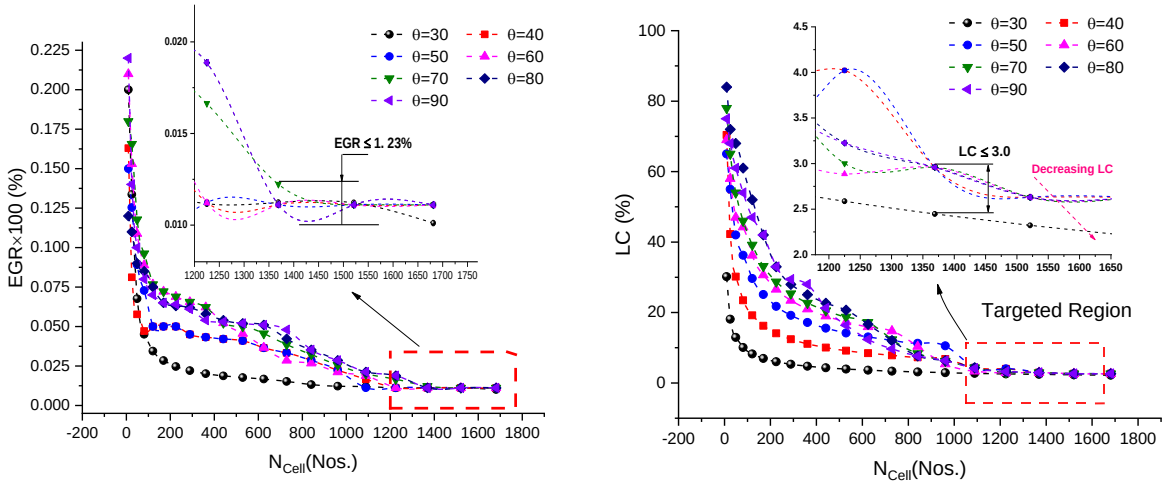

(a) (b)

Fig. 4 Zone of '*illusive convergence*' using; a) EGR method and b) LC method.

Chapter 3 Experimental model and CAD modelling of FPSRS

3.1 Experiment of STC area based FPSRS

The present section discusses the details of an experiment setup undertaken to investigate the optical behaviour of a typical FPSRS. Fig. 5 shows the schematic of the experimental setup. The experiment has been conducted in-house in the laboratory. The test setup consists of two vertical pillars between which a horizontal rectangular cross-section wooden bars is fixed. The arrangement of the bar is such that it is capable of holding laser light and at the same time it can be rotated to any desired angle. The effect of the movement of laser light on the horizontal bar can be best explained by the movement in either X or Y directions (refer Fig. 5) to facilitate the experiments. Fig. 6 shows the making of FPSRS and images of the setup to test the FPSRS in working condition. The set-up is arranged to slide above FPSRS as shown in Fig. 6 (f), allowing the laser light to be directed at any desired angle. FPSRS is made of four trapezoidal shaped reflectors.

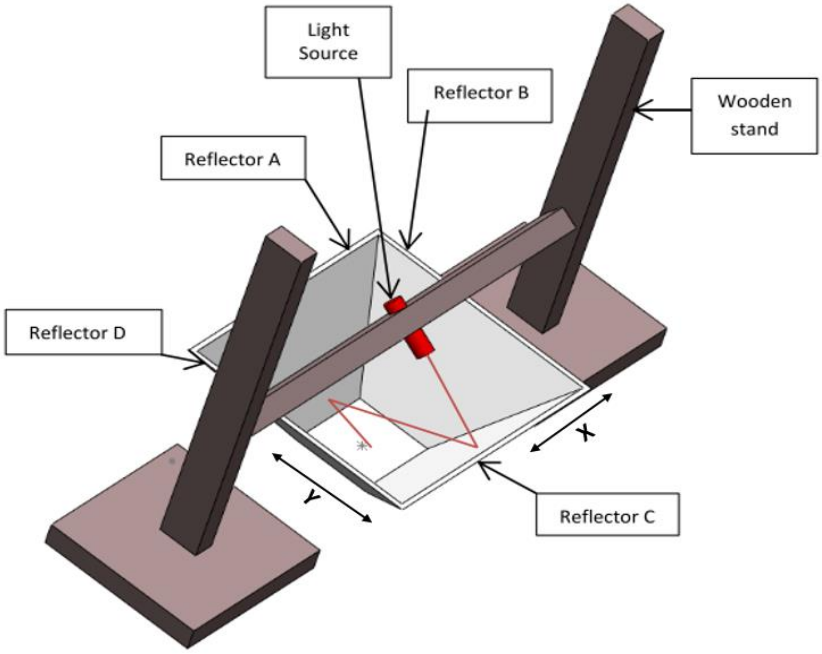

Fig. 5 Schematic of experimental set up with FPSRS and laser light in position.

3.2 Classification of rays and CAD modelling of FPSRS

In order to conduct a systematic analysis of the rays, the interaction of the ray with the reflector are classified into six different categories, based on their paths in the reflector geometry. The detailed classification is as displayed in Table 2. The use of this data is made to show the collector efficiency as discussed in the later section. The pictorial representation of all the different types of rays are shown in Fig. 6, while Fig. 7 shows case wise description of the travel of the similar ray during experiment. The all images in the Fig. 7 are observed little contrast due to the darkness of the experimental room. To identify the correct instance of reflection, out of many,

and overcome the issue of multiple reflection, a special arrangement in the set-up is made at the time of the experiments. Under this arrangement the entire surface of non-participating reflectors will be covered or hidden by means of a partially sliding opaque cover. For all the cases, the FPSRS setup up is assumed to be having azimuthal alignment, the reflector R3 will be facing the sun directly at all the angles, the red arrow in the Fig. 8 shows the direction of the sun ray (which will be as per the left to right direction). It is observed that full part of reflector R1 and a large portion of the reflector R2 and R4, especially bottom part, remain blank or having no occurrence of ray intersection. This is due to the reflector R1 actually blocking the most of the surfaces of the rest of the reflectors. Occurrence of direct ray reaching to BRS starts from 50◦ onwards and reaches maximum value at 90◦.

Table 2 Classification of rays' interaction with FPSRS

Case	Description
A	Rays reaching directly at the bottom receiver.
B	Rays reaching at bottom receiver after one reflection.
C	Rays reaching at bottom receiver after two reflections.
D	Rays reaching at the bottom receiver via reflection from a neighbouring reflector.
E	Rays never reaching at the bottom receiver even after multiple reflection.
F	Rays never reaching at the bottom receiver but quit the system after one reflection.

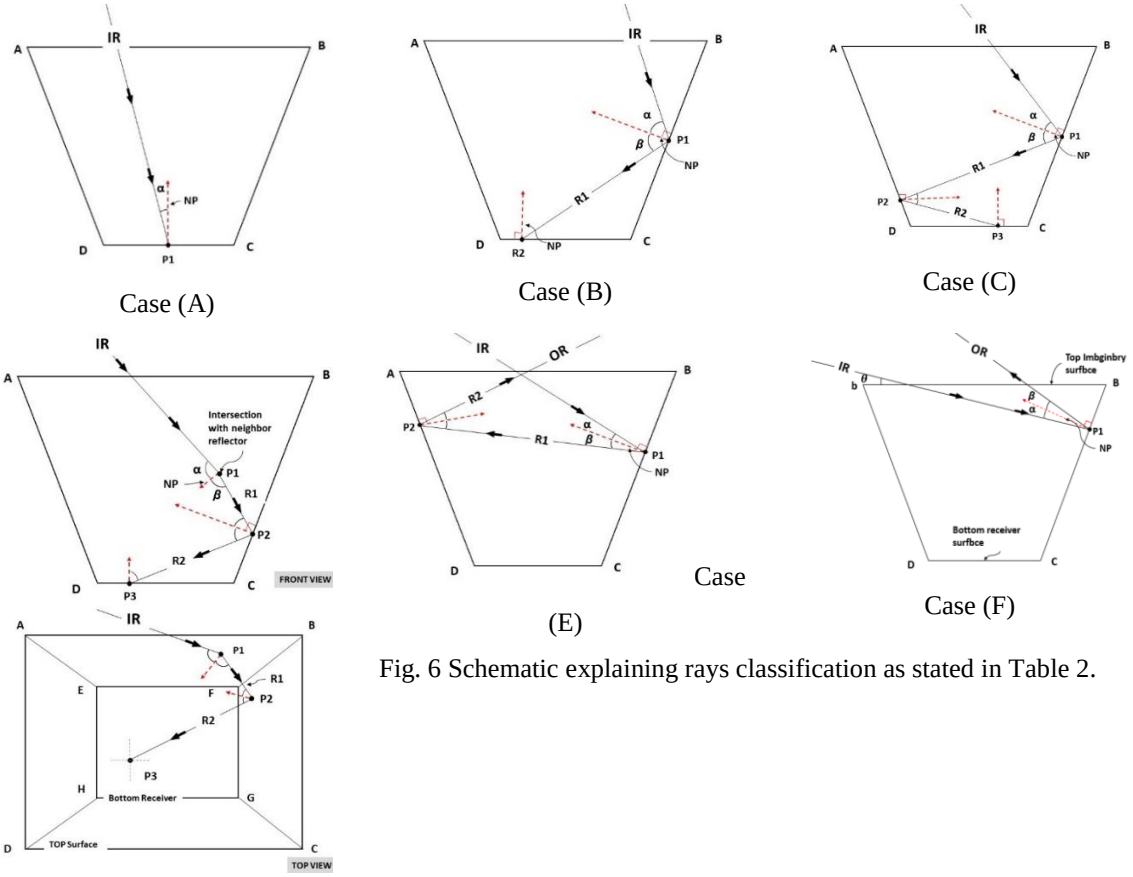

Case (A) Case (B) Case (C)

Case (D) Case (E) Case (F)

Fig. 6 Schematic explaining rays classification as stated in Table 2.

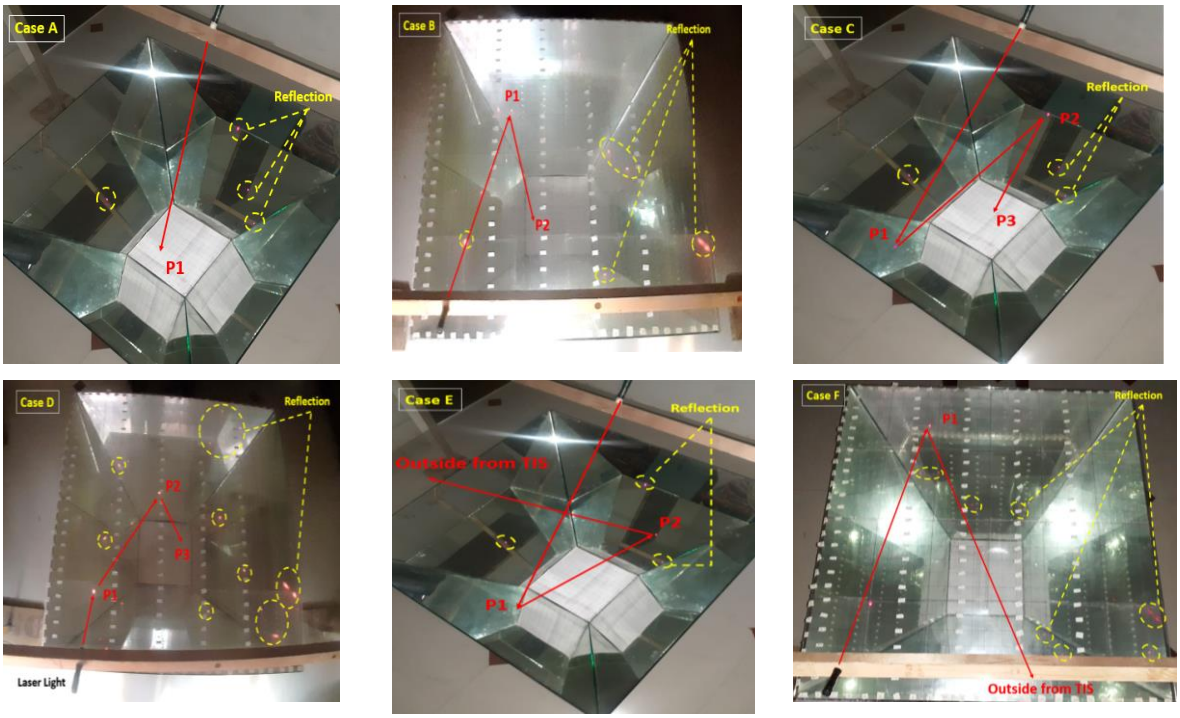

Fig. 7 Case wise representation of incident light beam reflection.

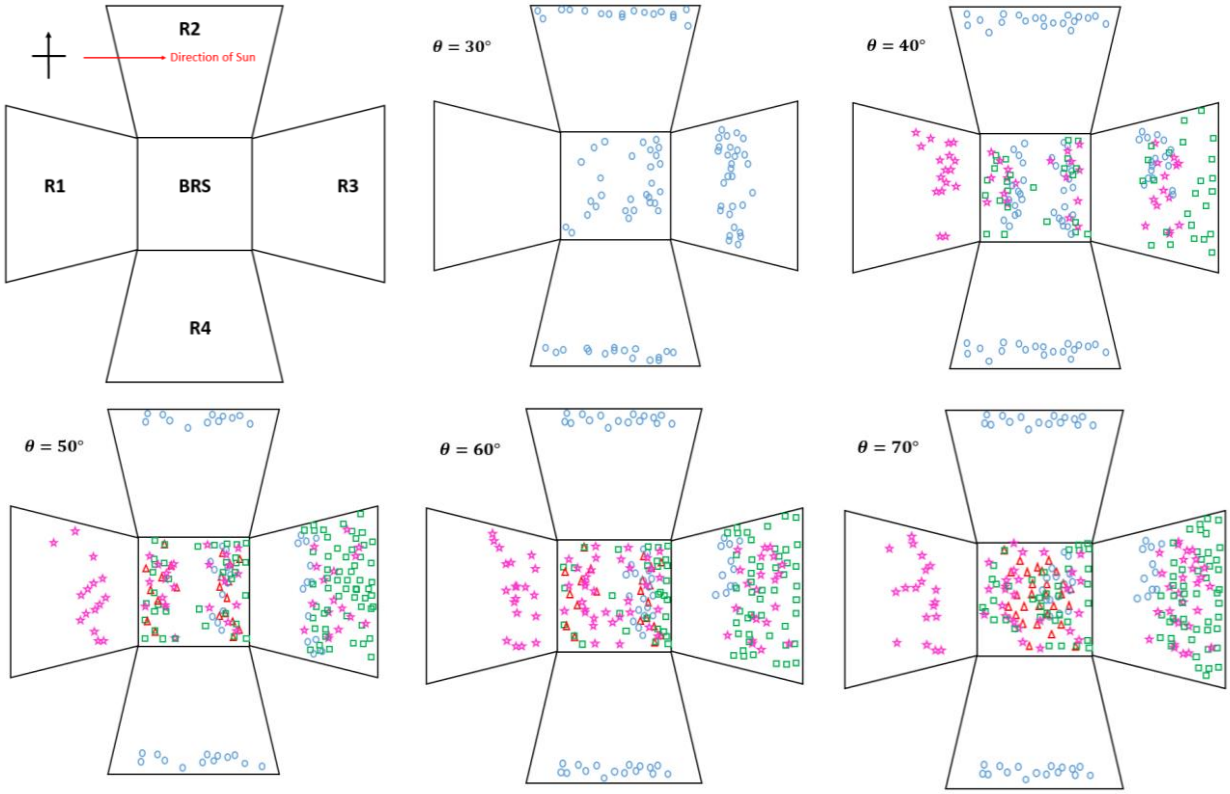

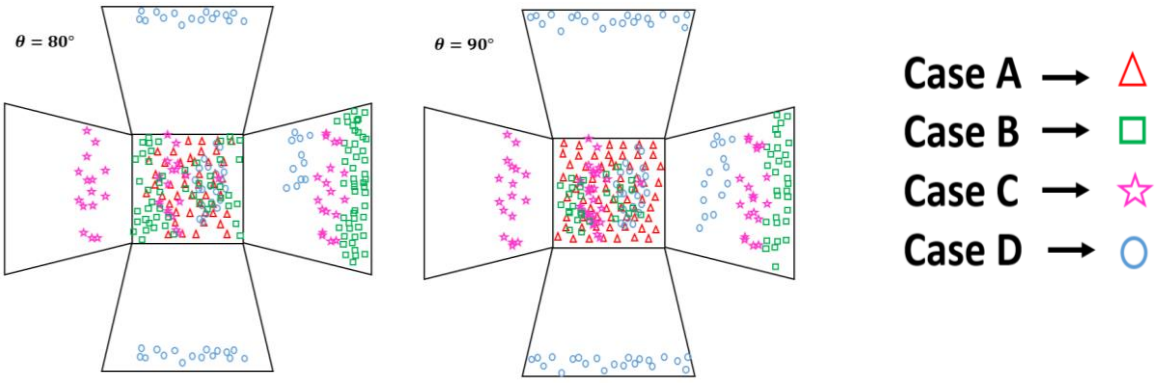

Fig. 8 Instances of occurrences of rays from A to D on the FPSRS for different solar incident angle.

3.3 Uncertainty analysis

For the mathematical equations (refer Eq. 15) the extreme uncertainty in experiment can be determined by Kline and Mcclintock method [15]. This method prescribed the total uncertainty ($\Delta\chi$) as a function of uncertainty present in the performance of single ray (n) behaviour. The error may be due to manufacturing or during cutting of the reflectors or error while joining of FPSRS. The error is covered under uncertainty error (χ). For this the error in angle of each side reflector, due to cutting or joining the reflector is considered as $\Delta\alpha_h$= 1° as maximum possible error. Fig. 9 depicts a schematic picture of the inaccuracy noticed when reducing and ascending in angle (slop of reflector). The ideal case as$\angle AOB = 60°$, and the actual case after considering error of -1◦ and +1◦, the angle becomes $\angle A'OB' = 58°$ (as shown in Fig. 9 (a)), and 62° (as shown in Fig. 9 (b)) respectively. The maximum uncertainty in both the cases (58° and 62°) are 2.90% + 2.96 % = 5.86% (for case D type ray) for the FPSRS which is high compared to other cases. This confirms the presence of non-additive nature of the error in case of experimental set-up. In spite of this, looking to the overall value of the uncertainty, one can conclude that a similar FPSRS unit can be a reliable solar reflector unit and can be suitably considered for large applications.

$$\Delta\chi = \sqrt{\left(\frac{\partial\chi}{\partial n_1}\cdot\Delta n_1\right)^2 + \left(\frac{\partial\chi}{\partial n_2}\cdot\Delta n_2\right)^2 + \cdots + \left(\frac{\partial\chi}{\partial n_n}\cdot\Delta n_n\right)^2} \quad (15)$$

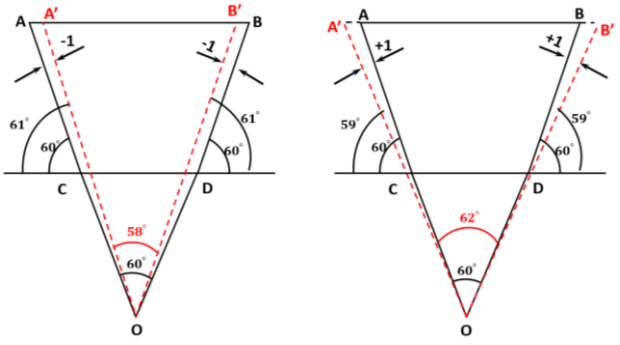

(a) **(b)**

Fig. 9 Two hypothetical reflectors pyramid angle; (a) reduced by (-1) and (b) increased by (+1)

Chapter 4 Results and discussion

4.1 Validation of the experimental results

Present section discusses the quantification of the error resulting from the experiment and its interpretation. It is essential to quantify the methods used to perform the experiment and the computed error as this will help validate the testing procedure followed and quantify its effectiveness. If error is under control the present method can be extended to analyse other types of reflector geometry as well, e.g. having TIS in the shape of hexagonal, octagonal, decagon, etc. First, the proposed single ray tracing experimental methodology is validated with the already performed experiment by A. C. Andre et al. [6] on funnel type of solar cooker with considering shadow type tracing methodology. The optical performance of the FPSRS is measured in the forum of ray distribution profile on the BRS and it can be obtained from Eq. 16. The Fig. 10 shows the results of comparative study for the optical performance of present experimental study and the experiments perform with consideration of shadow type tracing method. From the result it is observed that there is a good agreement between the results. Additionally, the error analysis is carried out by considering certain number of rays in each category of ray classification. For this total four number of the rays are considered in each class, i.e. A to F and these rays are considered for each different angles, i.e. 30◦ to 90◦. The deviation obtained is as per Eq. 17 and the result is summarised in the Table 3. It shows the summary of the result of the error analysis for FPSRS. It is observed that the maximum amount of error observed is 3.1% in Case-D type rays when the value of θ is 40°.

$$\text{RDP}(\%) = \frac{\text{No of rays reached at BRS}}{\text{No of ray on TIS}} * 100 \quad (16)$$

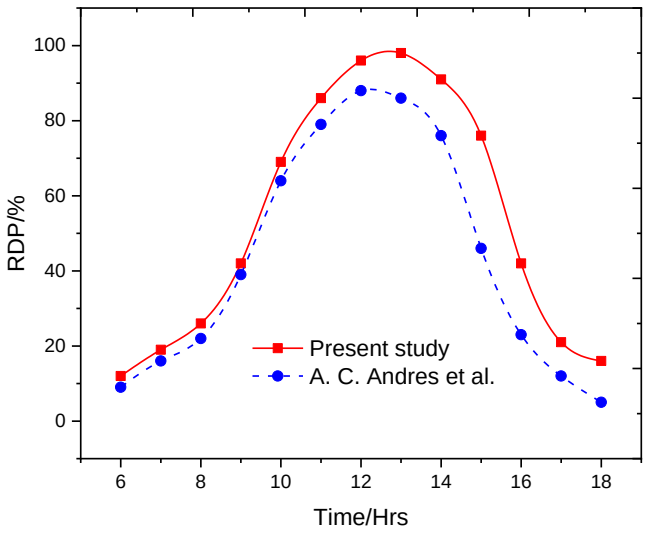

Fig. 10 Comparative study of the optical performance of present study and the experimental work [6]

$$\text{Error } (\delta_E) = \frac{|(\text{Coordinate from CAD model} - \text{Coordinate from experiment model})|}{Length\ of\ travel\ of\ the\ ray} \times 100 \quad (17)$$

Table 3 Value of δ_E (%) observed for the rays reaching to the BRS [min, max]

θ	N	Case A	Case B	Case C	Case D
30º	1 to 4	-- *	-- *	-- *	1.6, 2.1
40º	1 to 4	-- *	0.2, 2.1	0.4, 1.5	0.36, **3.1**
50º	1 to 4	0.2, 0.2	0.3, 2.1	0.8, 2.2	0.7, 1.1
60º	1 to 4	0.5, 0.5	0.2, 1.3	0.2, 2.1	0.5, 1.8
70º	1 to 4	0.3, 1.1	0.4, 1.2	0.2, 2.0	0.2, 2.1
80º	1 to 4	0.1, 0.4	0.4, 1.2	0.2, 1.5	0.4, 2.2
90º	1 to 4	0.1, 0.3	0.3, 0.8	0.2, 1.6	0.2, 1.1

Note: * The cases shown with the dashed lines represent the rays not successful in reaching at the bottom.

The comparative analysis between the RTA and experimental work for FPSRS is discuss in the following discussion. The experiment considered various factors, and despite slight discrepancies observed, the results show that the RTA remains a dependable tool, suitable for assessing similar aperture area based FPSRS systems. The validation of the RTA was conducted through experimental work performed by J. Patel et al. [16] on the STC based FPSRS. To ensure a meaningful comparative study, certain assumptions were made in line with the experimental investigation. Specifically, the number of incoming rays (N_{TIS}) were set to 576, and the input solar radiation data corresponded to the month of June 2020 at the location of Vadodara, Gujarat, India. The comparative results of two key parameters, namely, the RDP and optical efficiency (η_{opt}), were presented in Fig. 11(a) and 11(b), respectively. The η_{opt} can be obtained from Eq. 18 and the analysis of the results revealed a slight difference of 2.9% in the case of RDP and 3.2% in the case of optical efficiency. It is important to note that a significant portion of the observed variation in the results could be attributed to mechanical measurements and potential human errors while taking readings during the experiments. Based on these findings, it can be determined that the validation results are well-controlled, and the RTA demonstrates accuracy and reliability.

$$\eta_{opt} = \sum_{j=1}^{N_{TIS}} (I_{BRS} \cdot \delta_r^j) / I_{TIS} \quad (18)$$

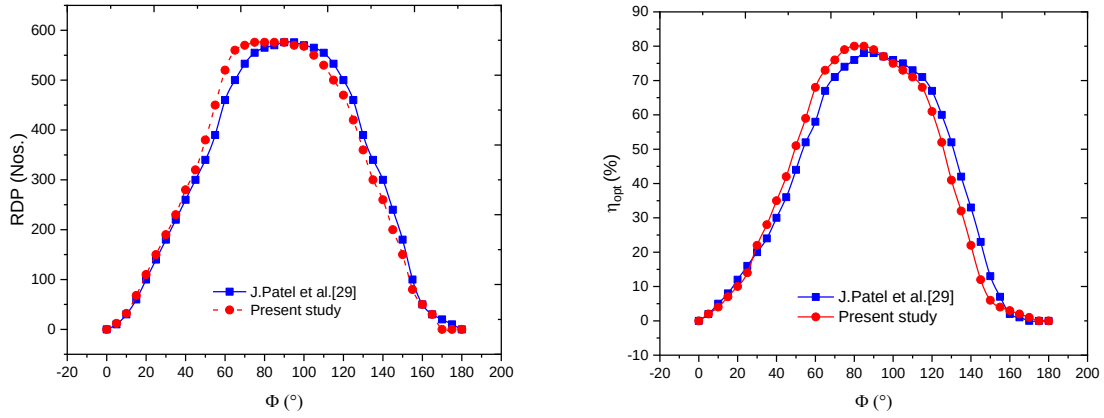

(a) (b)

Fig. 11 (a) and (b) illustrate a comparison between the experimental work and present study in terms of RDP andη_{opt}, respectively.

4.2 Topological optimisation of the FPSRS

The angular position of the flat plate reflector of FPSRS has a significant impact on the optical performance. The numerical investigation on a FPSRS with STC area has been conducted, and the impact of the value of different α_H on its optical performance has been analysed. By varying the ratio of vertical height (H) to the length of the square bottom receiving surface (B), the value of α_H can be changed. Summer solstice (SS) and winter solstice (WS) are two limiting conditions for which the entire study is conducted. The ray's reflection process and its final location on the BRS or leaving from the TIS is reported. The effect of the H/B ratio on the optical performance of the STC based FPSRS is shown Fig. 12. The findings suggest that the overall RDP is gave optimum output in SS atmospheric conditions when H/B is 2, but the RDP is optimum in WS atmospheric conditions when H/B is 1.52. Consequently, the current system's optical performance will be better in both environmental conditions at the default H value of 0.38 m, but it can perform at its peak when H is 0.5 m, particularly for SS conditions.

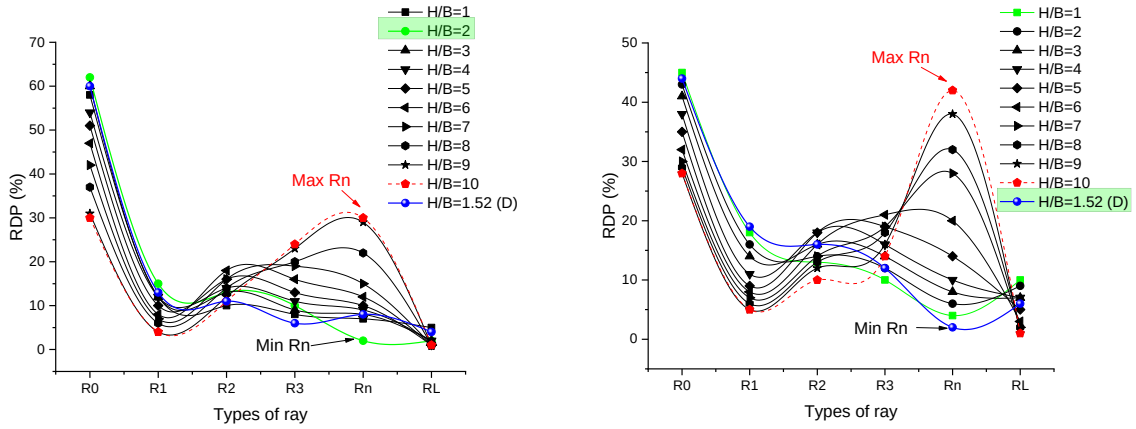

(a) SS (b) WS

Fig. 12 RDP with different value of H/B for two different extreme atmospheric condition.

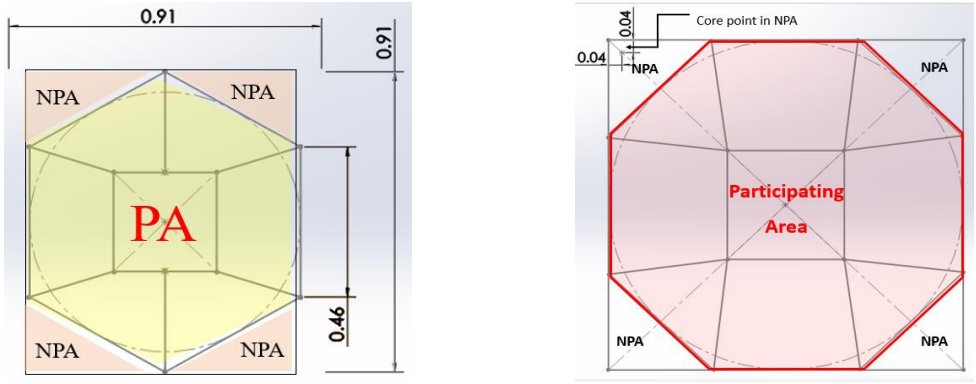

(a) (b)

Fig. 13 Participating area (PA) and Non participating area (NPA) for HTC and OTC based FPSRS.

Additionally, the effect of the STC, HTC and OTC on the optical performance of the FPSRS is analysed with using RTA. The STC, HTC and OTC based FPSRS is analysed. The participating area (PA) and non-participating area (NPA) for HTC and OTC based FPSRS is shown in Fig. 13 (a) and Fig. 13 (b), respectively. The results is

presented in the forum of six alternative classifications of the ray have been created based on the ways of ray reflection with reflectors. The optical performance of the STC and OTC based solar reflective systems are compared. Lastly, by taking into account the solar radiation of the four different locations of India, the impact of solar altitude angle on the performance of the reflecting system is studied. The comparative results for the different type of aperture area based FPSRS is obtained and it is observed that OTC and HTC based geometry gave better results compared to STC based system. However, in the case of OTC and HTC based system, the OTC based system is out performed and the average value of RDP for it is 5.1 % more compared to HTC based system.

Chapter 5 Conclusion and future scope

5.1 Conclusion

The flat plate reflectors are reasonably priced, widely accessible, and locally produced. Despite having all of these positive traits, there is a significant efficiency loss when compared to their curved counterparts, which necessitates researcher to determine the best economic option for a scaled-up thermal application. This study assesses FPSRS optical performance using a customized approach to track single rays, categorized into six groups from case A to case F. Experiments involved a flat plate solar reflecting system in a dark room directing laser light onto FPSRSs at varying incidence angles. Numerical investigations explored the impact of BRS height-to-base ratios and different aperture areas on FPSRS optics. A tailored RTA was developed to analyse diverse topological combinations, with ensuing outcomes discussed in the following section.

- The single-ray experimental findings align with A. C. Andres et al.'s [6] earlier shadow experiment and The validated outcomes demonstrated that the currently proposed experimental procedure is both more reliable and feasible than traditional approaches. The experimental setup was corroborated by modelling it in CAD software, and the path of rays and their intersecting coordinates on the reflector closely matched. Notably, the highest discrepancy between the experimental and CAD software results was found in case D, amounting to 2.1%.
- The RDP results show that the contribution of rays from case A and case B increases significantly with θ angle between 60° and 90°, enhancing the system's overall efficiency (η_C). The documented overall uncertainty effect indicates that the maximum uncertainty remains below 5.8%. In practical applications, this uncertainty will decrease significantly as the FPSRS size scales up, being 4 to 5 times larger than the experimental model.
- In SS and WS atmospheric conditions, the most significant RDP values for STC area-based FPSRS occurred at 53° to 58° reflector angles for H/B ratios of 2 and 1.52, respectively.
- Results indicate that the HTC-based FPSRS achieves a significantly higher η_{opt}, outperforming the STC-based system by 15%, highlighting its geometric advantages. Conversely, OTC surpasses STC in RDP performance. Both HTC and OTC systems efficiently convert type E and F rays to type C and predominantly type D, resulting in a remarkable 23% reduction in exiting rays compared to STC-based configurations. In comparison, OTC based FPSRS outperforms STC area-based systems by 5.1% in optical efficiency.

The results of this numerical investigation underscore the importance of aperture shape in shaping the optical efficiency of the FPSRS. The OTC configuration outperformed both the HTC and STC configurations. These insights advance solar energy technology and assist in designing and optimizing solar reflecting systems to improve energy capture and utilization.

5.2 Future scope

In the wake of this research, several promising avenues for future exploration emerge. Firstly, there is a clear need to delve deeper into the realm of advanced aperture designs. As this study highlights the pivotal role of aperture shape in optimizing the optical performance of FPSRSs, further investigations can focus on the development of innovative aperture designs. This includes exploring novel shapes and configurations that can augment the efficiency of FPSRSs, ultimately improving their ability to capture and concentrate solar energy effectively. Another promising direction for future research lies in the realm of manufacturing innovation. While flat plate FPSRSs offer cost-effective advantages, the manufacturing complexity associated with curved reflectors remains a substantial challenge. Future endeavours could concentrate on devising innovative manufacturing solutions. Developing scalable and cost-efficient processes for both flat plate and curved reflectors can significantly impact their accessibility and affordability, making high-performance solar reflectors more attainable on a broader scale.

The integration of FPSRSs with energy storage technologies represents a captivating avenue for future research. Investigating seamless integration with advanced thermal storage or innovative photovoltaic systems can enhance the harnessing and utilization of solar energy. This not only increases the economic viability of solar thermal applications but also contributes to the reliability and sustainability of renewable energy solutions. Moreover, multi-objective optimization techniques should be explored in depth. Achieving a balance between optical efficiency, cost-effectiveness, and environmental considerations is a complex challenge. Future research can delve into methodologies for finding optimal trade-offs among these factors. This could lead to the development of solar energy systems that are not only highly efficient but also economically and environmentally sustainable. Lastly, expanding the geographic scope of research to assess FPSRS performance under diverse solar radiation conditions and in various regions worldwide holds significant potential. This global perspective can contribute to the development of tailored solutions for specific environments and climates, promoting the widespread adoption of FPSRSs and sustainable energy practices on a global scale.

5.3 Research outcomes

Present section discuss about the publication published/ under review relevant to present research work.

Journal publication:

(1) Jay Patel, Amit R Patel, Chintan Mulasiya, “Determination of optical and thermal performance of a large - sized flat plate solar reflector unit under azimuthal sun alignment”, Journal of Thermal Analysis and Calorimetry, Springer publication, 148, 8991–9011 (**2023**). https://doi.org/10.1007/s10973-023-12282-2. (Impact Factor: **4.7**/ **SCI**)

(2) Jay Patel, Amit R Patel, “Study on the effect of different types of aperture area on the optical performance of solar flat plat reflecting system”, Sustainable Energy Technology and Assessment, Elsevier, Science direct. (**Under review**/ Impact Factor: **8.0**/ **SCI**)

(3) Jay Patel, Amit R Patel, "Methods and guidelines for determining optimum grid number with considering space and time-dependent problem using ray tracing algorithm for solar reflecting system", Sustainable Energy Technology and Assessment, Elsevier, Science direct. (**Under review**/ Impact Factor: **8.0/ SCI**)

Conference publication:

(1) Jay Patel, Amit R Patel, "Numerical investigation on the effect of different types of aperture area on the optical performance of solar flat plat reflecting system", International conference on environmental sustainability (ICES), VJTI, Matunga, Maharashtra. **(March 2023)**

(2) Jay Patel, Amit R Patel, "Effect of reflector height to base ratio on the optical performance of square shaped aperture area based flat plat solar reflecting system", International Conference on Recent Advances in (Applied) Sciences & Engineering (RAISE), MSU, Baroda, Gujarat. **(April 2023)**

(3) Jay Patel, Amit R Patel, "Effect of octagonal shaped aperture area on optical performance of the simple flat plate solar reflecting system", 1st IEEE international conference on renewable energy and sustainable E- mobility, MNIT, Bhopal, M.P. **(May 2023)**

Book chapter:

(1) Jay Patel, Amit R Patel, "Recent advancements in large-scale solar flat plate reflecting systems: Their analysis with unique analytical technique, application, scaling up strategies, and economics as they are applied to underdeveloped countries", Title: The costs of climate change mitigation innovation- A pragmatic outlook, editor: Dr. D. Ting, Dr. J. Stagner, Taylor & Francis publication. **(Dec, 2023)**

Patent:

(1) Jay Patel, Amit R Patel, "Prediction of solar beam ray with use of ray tracing algorithm for flat plate type reflector", **waiting for funding.**

References:

[1] M. A. R. Ibrahim Dincer, *Thermal Energy Storage system and applications*, 2nd ed. Onterio,Canada: A John Wiley and sons, Ltd., Publication, 2011.

[2] D. F. Birol, "International Energy Agency (IEA)," *Word Energy Outlook*, 2021. www.iea.org/weo (accessed Jun. 01, 2023).

[3] B. K. Naik, M. Bhowmik, and P. Muthukumar, "Experimental investigation and numerical modelling on the performance assessments of evacuated U – Tube solar collector systems," *Renewable Energy*, vol. 134, pp. 1344–1361, 2019, doi: 10.1016/j.renene.2018.09.066.

[4] Y. Zhu, J. Shi, Y. Li, L. Wang, Q. Huang, and G. Xu, "Design and thermal performances of a scalable linear Fresnel reflector solar system," *Energy Conversion and Management*, vol. 146, pp. 174–181, 2017, doi: 10.1016/j.enconman.2017.05.031.

[5] C. R. Ruivo, A. Carrillo-Andrés, and X. Apaolaza-Pagoaga, "Experimental determination of the standardised power of a solar funnel cooker for low sun elevations," *Renewable Energy*, vol. 170, pp. 364–374, 2021, doi: 10.1016/j.renene.2021.01.146.

[6] A. Carrillo-Andrés, X. Apaolaza-Pagoaga, C. R. Ruivo, E. Rodríguez-García, and F. Fernández-Hernández, "Optical characterization of a funnel solar cooker with azimuthal sun tracking through ray-tracing simulation," *Solar Energy*, vol. 233, no. August 2021, pp. 84–95, 2022, doi: 10.1016/j.solener.2021.12.027.

[7] William Bradley, "Reciprocal Optical Test for Measuring solar Cooker Performance," *Earthboundtech.com*, pp. 1–20, 2012, [Online]. Available: https://www.earthboundtech.com/optical-test

[8] H. M. Wassie, M. Z. Getie, M. S. Alem, T. B. Kotu, and Z. M. Salehdress, "Experimental investigation of the effect of reflectors on thermal performance of box type solar cooker," *Heliyon*, vol. 8, no. 12, p. e12324, 2022, doi: 10.1016/j.heliyon.2022.e12324.

[9] A. S. Abdullah, M. I. Amro, M. M. Younes, Z. M. Omara, A. E. Kabeel, and F. A. Essa, "Experimental investigation of single pass solar air heater with reflectors and turbulators," *Alexandria Engineering Journal*, vol. 59, no. 2, pp. 579–587, 2020, doi: 10.1016/j.aej.2020.02.004.

[10] H. Bhowmik and R. Amin, "Efficiency improvement of flat plate solar collector using reflector," *Energy Reports*, vol. 3, pp. 119–123, 2017, doi: 10.1016/j.egyr.2017.08.002.

[11] H. Tanaka, "Theoretical analysis of solar thermal collector and flat plate bottom reflector with a gap between them," *Energy Reports*, vol. 1, no. April, pp. 80–88, 2015, doi: 10.1016/j.egyr.2014.10.004.

[12] S. S. More, G. Ravindranath, S. E. More, and S. S. Thipase, “Mathematical modeling and analysis of compound parabolic concentrator using soltrace,” *International Journal of Mechanical Engineering and Technology*, vol. 9, no. 6, pp. 113–121, 2018.

[13] Q. Chen and J. Srebric, “A Procedure for Verification, Validation, and Reporting of Indoor Environment CFD Analyses,” *HVAC&R Research*, vol. 8, no. 2, pp. 201–216, Apr. 2002, doi: 10.1080/10789669.2002.10391437.

[14] N. Kumar Adichwal, A. Ali H. Ahmadini, Y. Singh Raghav, R. Singh, and I. Ali, “Estimation of general parameters using auxiliary information in simple random sampling without replacement,” *Journal of King Saud University - Science*, vol. 34, no. 2, p. 101754, Feb. 2022, doi: 10.1016/j.jksus.2021.101754.

[15] S. J. Kline, “The purposes of uncertainty analysis,” *Journal of Fluids Engineering, Transactions of the ASME*, vol. 107, no. 2, pp. 153–160, 1985, doi: 10.1115/1.3242449.

[16] J. Patel, A. R. Patel, and C. Mulasiya, “Determination of optical and thermal performance of a large - sized flat plate solar reflector unit under azimuthal sun alignment,” *Journal of Thermal Analysis and Calorimetry*, pp. 1–21, 2023, doi: 10.1007/s10973-023-12282-2.